

All-sky Observations with Suzaku Wide-band All-sky Monitor and MAXI

M. Ohno,¹ M. Kokubun,¹ T. Takahashi,¹ K. Yamaoka,² M. Serino,³
Y. E. Nakagawa,³ T. Tamagawa,³ Y. Fukazawa,⁴ T. Uehara,⁴ Y. Hanabata,⁴
T. Takahashi,⁴ S. Sugita,⁵ N. Vasquez,⁶ Y. Terada,⁷ M. Tashiro,⁷
S. Hong,⁷ W. Iwakiri,⁷ K. Takahara,⁷ T. Yasuda,⁷ N. Ohmori,⁸ A. Daikyujji,⁸
Y. Nishioka,⁸ M. Yamauchi,⁸ Y. Urata,⁹ P. Tsai,⁹ K. Nakazawa,¹⁰ K. Makishima,¹⁰
and the Suzaku-WAM team and MAXI team

¹ Institute of Space and Astronautical Science, Japan Aerospace Exploration Agency,
3-1-1 Yoshinodai, Chuo-ku Sagamihara, Kanagawa 252-5120, Japan

² Department of Physics and Mathematics, Aoyama Gakuin University,
5-10-1 Chuo-ku Fuchinobe, Sagamihara, Kanagawa 252-5258, Japan

³ The Institute of Physical and Chemical Research (RIKEN),
2-1 Hirosawa, Wako, Saitama 351-0198, Japan

⁴ Department of Physics, Hiroshima University,
1-3-1 Kagamiyama, Higashi-Hiroshima, Hiroshima 739-8516, Japan

⁵ Division of Energy Science, EcoTopia Science Institute, Nagoya University,
Furo-cho, Chikusa-ku, Nagoya 464-8603

⁶ Department of Physics, Tokyo Institute of Technology,
2-12-1, O-Okayama, Meguro, Tokyo 152-8551, Japan

⁷ Department of Physics, Saitama University,
255 Shimo-Okubo, Sakura-ku, Saitama-shi, Saitama 338-8570, Japan

⁸ Department of Applied Physics, University of Miyazaki,
1-1 Gakuen Kibanadai-nishi, Miyazaki-shi, Miyazaki 889-2192, Japan

⁹ Institute of Astronomy, National Central University, Chung-Li 32054, Taiwan

¹⁰ Department of Physics, University of Tokyo, 7-3-1 Hongo, Bunkyo-ku, Tokyo 113-0033, Japan

E-mail(MO): ohno@astro.isas.jaxa.jp

ABSTRACT

All-sky observation in wide energy band is important to study bright gamma-ray sources as well as other transient phenomena such as Gamma-ray Bursts (GRBs). Suzaku Wide-band All-sky Monitor (WAM) enables such all-sky observations up to soft gamma-ray band thanks to its wide energy coverage from 50 keV to 5000 keV with very large effective area of 400 cm² even at 1 MeV. During five year operations, any serious detector problems have not come up and the WAM has successfully detected more than 750 GRBs. Simultaneous detection between the WAM and MAXI of GRB 090831A is an example of a GRB spectroscopy in wide energy range from a few keV to MeV. In addition, the WAM is monitoring many bright gamma-ray sources such as Crab and Cyg X-1 by utilizing the earth occultation technique. Cooperation between the WAM, MAXI, and other all-sky instruments enables us to compare the behavior of their light curves in X-ray and soft gamma-ray energy band.

KEY WORDS: gamma rays: observations

1. Introduction

In the hard X-ray band (> 10 keV), non-thermal processes begin to take an important role for the emission and there are many bright astronomical object in that energy band such as Gamma-ray Bursts (GRBs), soft gamma-ray repeaters (SGRs), black hole or neutron star binaries, solar flares, and terrestrial gamma-ray flashes (TGFs). Therefore, monitoring all-sky in hard X-ray

band is very important to study non-thermal processes in the various sites in the universe. The Burst and Transient Source Experiment (BATSE) aboard the Compton Gamma-ray Observatory (CGRO) is the largest wide-field all-sky monitor with the energy band from 20 keV to about 1 MeV. Detection of many GRBs by BATSE brought important progresses of our knowledge for GRBs. Recently, the hard X-ray observations per-

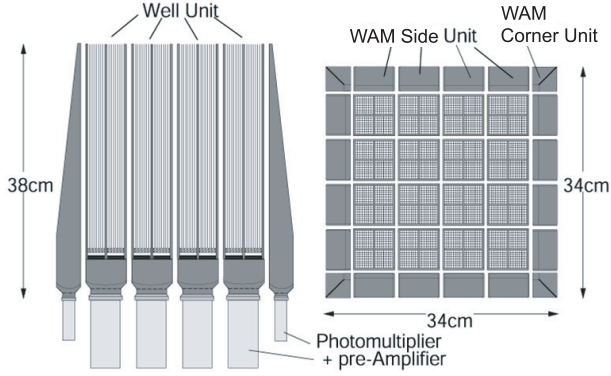


Fig. 1. Schematic view of the Hard X-ray Detector. Left: cross-section view. Right: Top view

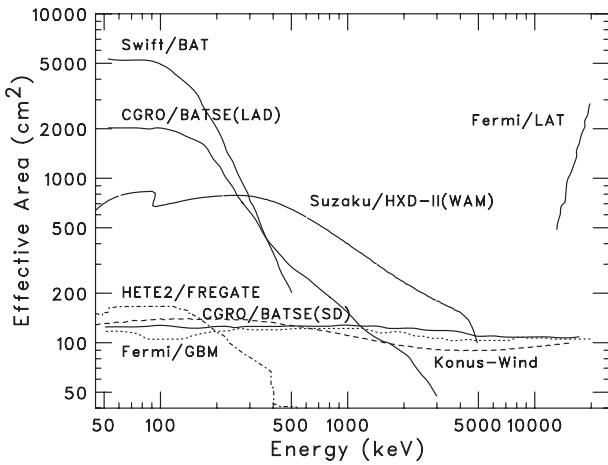


Fig. 2. Comparison of effective area of the WAM with previous and current all-sky instruments.

formed by Burst Alert Telescope (BAT; Gehrels et al. 2004) aboard Swift and high energy gamma-ray observations by Fermi (Atwood et al. 2009, Meegan et al. 2009) continue to provide new discoveries, and therefore, monitoring all-sky in hard X-ray band remains an important field in astronomy. Suzaku is the Japanese 5th X-ray astronomical satellite (Mitsuda et al. 2007). In addition to two main instruments aboard Suzaku, it also has a capability of monitoring all-sky in very wide energy coverage from 50 keV to 5 MeV with the largest effective area above 300 keV than any other all-sky instruments. In this paper, we report the current status of all-sky observation by Suzaku and discuss synergy between Suzaku and other all-sky instruments such as MAXI.

2. Suzaku Wide-band All-sky Monitor (WAM)

The Hard X-ray Detector (HXD; Takahashi et al. 2007), which is one of two narrow-field instruments onboard Suzaku satellite is surrounded by very large 20 BGO crystals as shown in figure 1. The primary role of these

Table 1. Characteristics of the Suzaku Wide-band All-sky Monitor

Energy range	50 keV – 5000 keV
Field of view	$\sim 2\pi$
Geometrical area	800 cm ²
Effective area	400 cm ² at 1 MeV
Energy resolution	$\sim 30\%$ at 662 keV
Time resolution	1 s (Transient data) 15.625 msec (GRB data)

BGO crystals is to serve main detector as an active shield for main detector. These BGO crystals has very large effective area over very wide energy band thanks to their geometrically large and thick structure composed by high-Z ($Z_{\text{eff}} = 71$ for BGO) materials. In addition, such surrounding configuration for the main detector realizes very wide field of view ($\sim 2\pi$ str). Therefore, we can use these BGO crystals not only as active shield for the main detector but also as all-sky monitor with large effective area covering the energy band from 50 keV to 5 MeV. This is called as Wide-band All-sky Monitor (WAM; Yamaoka et al. 2009). As shown in figure 2, the WAM has the largest effective area above 300 keV compared with any other all-sky instruments which has a capability of measuring spectrum. Table 1 summarizes the characteristics of the WAM. All-sky observations by the WAM can provide us a wide-band spectroscopy from hard X-ray to soft gamma-ray band with a good photon statistics for GRBs, SGRs, and solar flares. In addition to such transient phenomena, the WAM can monitor the bright hard X-ray sources such as Crab and Cyg X-1 by utilizing earth occultation technique.

2.1. Current status

During about 5.4 years operation, (from August 2005 to December 2010), any serious operational problems have not come up. Table 2 shows the event list of the WAM. More than 800 GRBs have been detected by the WAM, and this means that the GRB detection rate of the WAM is about 150 GRBs per year. The WAM data also contributes to the localization of GRBs by joining the Inter Planetary Network (IPN). We successfully issued 166 GCN circulars to report the quick result of the WAM spectral analysis (130 circulars) and IPN localization (36 circulars). Figure 3 shows the duration (T_{90}) distribution of all detected GRB by the WAM. The bimodal distribution which is reported by BATSE (Paciesas et al. 1999) still can be seen by the WAM detected GRBs.

2.2. Calibration status

The energy response of the WAM is very complicate because the WAM is installed inside the satellite body and incident gamma-rays suffer heavy absorption due to the

Table 2. WAM event list from Aug. 2005 to Dec. 2010

confirmed GRB	804 (493)
possible GRB	449 (202)
SGR	378 (15)
solar flare	211 (30)

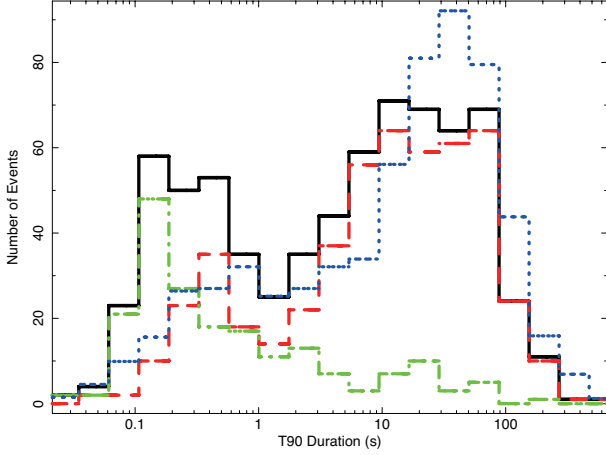


Fig. 3. T_{90} duration distribution of WAM detected GRBs from August 2005 to December 2009. Solid line shows the distribution of the confirmed and possible GRBs, Dashed-line shows that of confirmed GRBs, Dashed-Dotted line shows that of possible GRBs. The normalized distribution obtained by the BATSE 4B catalog (Paciesas et al., 1999) is also shown by the dotted line.

various materials on the satellite panels. Therefore, the energy response of the WAM strongly depends on the incident direction of the photon and we utilize the Monte Carlo simulation to calculate the detector response for all incident direction of each object. We have two kinds of procedures to calibrate the detector response of the WAM in orbit. One is the cross calibration using GRBs. We use simultaneously detected GRBs by the WAM, Swift-BAT, and Konus-Wind as a spectral calibration source. We compared spectral fitting results each other. Figure 4 shows the comparison of E_{peak} between the result from Konus-Wind with the result from joint spectral analysis between the WAM and Swift-BAT. From this GRB cross calibrations, we found that the spectral parameters of the WAM obtained in > 150 keV band agree within 20-30 % with other instruments. (Sakamoto et al. arXiv1011.1301). Another procedure is Crab calibration. We can extract the Crab spectrum by earth occultation technique as was performed by the BATSE (Harmon et al. 2002). The extracted spectrum is well fit by single power-law model with a photon index of ~ 2.1 and the energy flux in 100 to 500 keV energy band of $\sim 1.0 \times 10^{-8}$ erg cm $^{-2}$. These spectral parameters are roughly consistent with other gamma-ray instruments

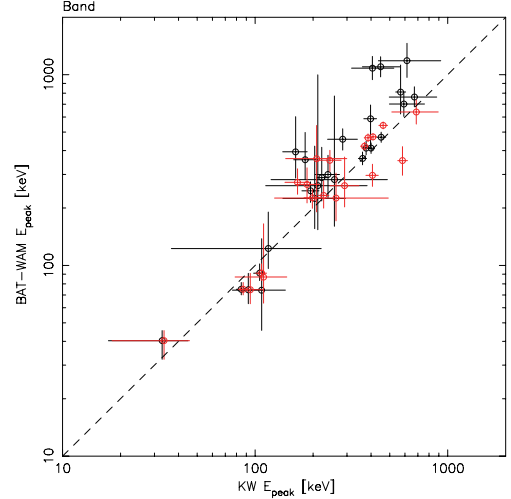


Fig. 4. Comparison of the E_{peak} obtained by the WAM-BAT joint spectral fitting with that of obtained by analysis using only Konus-Wind for the simultaneously detected GRBs.

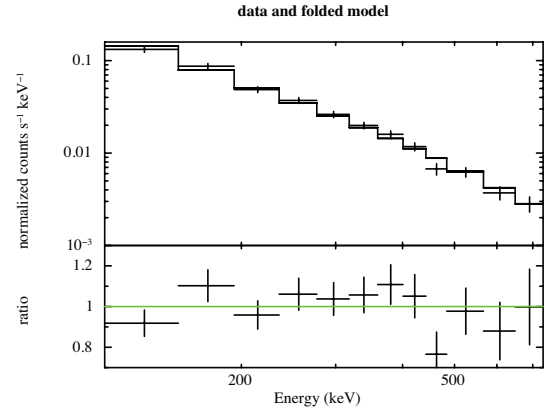


Fig. 5. The WAM Crab spectrum obtained by the earth occultation technique integrating 3-year observation data. Solid-line shows the best fit power-law model.

(Kira et al. 2009). From these in-orbit calibrations, we conclude that the current uncertainty of the energy response of the WAM is 20-30 % in > 150 keV energy band for almost cases. This uncertainty is consistent with our expectation based on the pre-flight calibrations (Ohno et al. 2005).

3. Spectral correlations of GRBs

Various spectral correlations have been suggested from previous GRB observations such as $E_{\text{peak}} - E_{\text{iso}}$ correlation (Amati relation; Amati et al. 2002), $E_{\text{peak}} - L_{\text{iso}}$ correlation (Yonetoku relation; Yonetoku et al. 2004). Such spectral correlations should be important to investigate the gamma-ray emission mechanism of GRBs. The WAM is very powerful to examine those correlations not only for each GRB but also time-resolved spectra

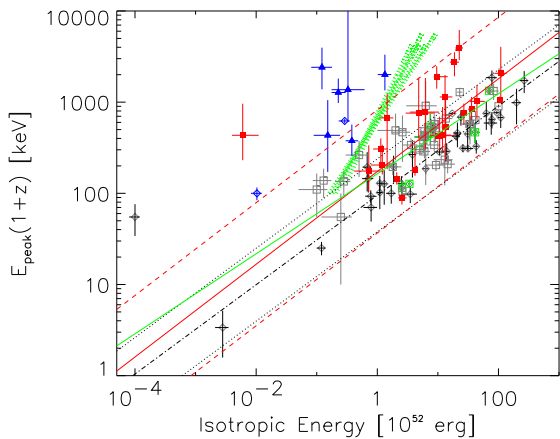


Fig. 6. $E_{\text{peak}} - E_{\text{iso}}$ correlation obtained by WAM-BAT joint spectral analysis (filled symbols) in comparison with previous sample (open symbols; Amati et al. 2006). Filled-squares and Filled-triangles are long and short GRBs from WAM-BAT sample, respectively. Open squares and Open diamonds are the bursts which are detected or not detected by Swift, respectively. Solid line is the fit to this data set. Detailed explanation for this figure is also found in Krimm et al. (2009)

within GRBs thanks to its very large effective area. In addition, since it became to measure the redshift even for short GRBs in the Swift era, we can investigate the differences of such correlations between short and long GRBs. Krimm et al. (2009) performed the joint spectral analysis between Swift-BAT and the WAM for 86 samples and examined $E_{\text{peak}} - E_{\text{iso}}$ correlation for the long and short GRBs. They found that most of WAM-BAT samples except for short GRBs also follow the same $E_{\text{peak}} - E_{\text{iso}}$ correlation obtained by previous analysis. On the other hand, all short GRB sample does not follow that correlation due to large E_{peak} value. This might reflect the differences of the origin between short and long GRBs. The $E_{\text{peak}} - L_{\text{iso}}$ correlation for the pulse-resolved spectra is examined by Sugita (2009) and the significant correlation was reported. This $E_{\text{peak}} - L_{\text{iso}}$ correlation was also confirmed even for time-resolved spectra within each pulse by Ohno et al. (2009) and Yamaoka et al. (in prep). They found that all of time-resolved spectra also follows similar correlation ($E_{\text{peak}} \propto L_{\text{iso}}^{0.5}$) but normalization parameter is different by the pulses or pulse phases (rising or decay phase). This result indicates that the such time-resolved analysis could be a probe to investigate the physical condition of emission region of GRBs.

4. Results from transient sources

The WAM also detected many transient sources other than GRBs and taking advantage of large effective area, the WAM data provides many interesting results. For SGR, more than 250 SGR flares have been observed from

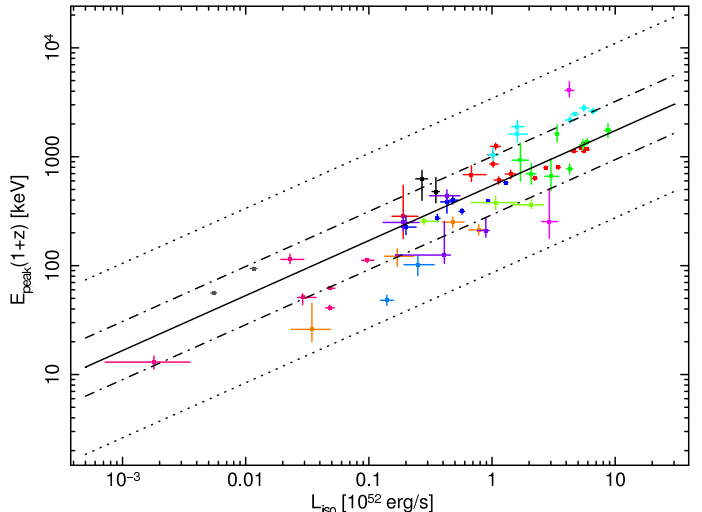


Fig. 7. $E_{\text{peak}} - L_{\text{iso}}$ correlation for pulse-resolved spectra obtained by WAM, BAT and HETE-2 sample. (Sugita 2009)

outburst of AXP 1E1547.0-5408 on January 2009 and discovered MeV photons for one flare spectrum. Detailed description for this SGR can be found in Yasuda et al. in this volume.

The WAM also detected many solar flares as shown in table 1. Thus, we developed a catalog of solar flares between July 2005 and November 2009 (Endo et al. 2010). 105 solar flares were detected by the WAM during this period. In this catalog, information of duration, peak count, photon index, flux in 100 keV, etc. is included. From this catalog, a weak trend that the events with longer durations exhibit harder spectral slopes was suggested.

5. Synergy between WAM and MAXI

As described above, Suzaku-WAM is a very powerful all-sky monitor in the energy band from 50 keV to 5 MeV, where non-thermal process begins to dominant for the emission. On the other hand, MAXI-GSC covers softer energy band than the WAM from 2 to 30 keV, where different processes such as thermal radiation are also contributed for the emission. Therefore, synergy between WAM and MAXI provides wider picture of the emission mechanism of gamma-ray sources covering both thermal and non-thermal regime.

5.1. Gamma-ray Bursts

Combination of GRBs with MAXI, WAM and other instruments provides us the GRB spectrum down to soft energy band and we could investigate a behavior of soft photons from GRBs. Although the MAXI can not observe many GRBs compared with other wide-field-of-view instruments, MAXI detected 16 events during 16 months observations and 8 out of 16 events have been

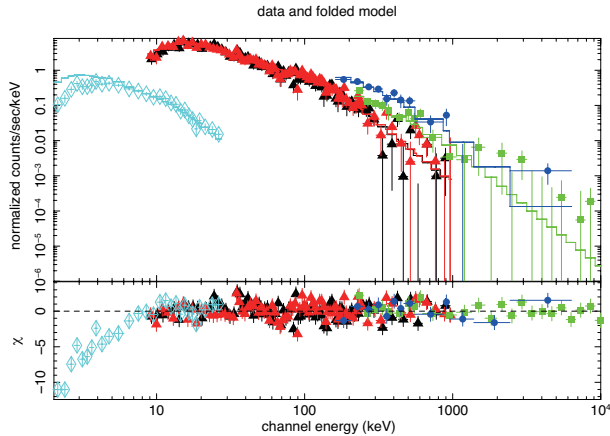


Fig. 8. Wide-band spectrum of GRB 090831A. Open diamonds are the MAXI-GSC, filled triangles are NaI detectors of GBM, filled squares are BGO detector of GBM, and filled circles are the WAM data. The best-fit model obtained by the WAM-GBM joint spectral fitting are also shown by the solid lines.

classified as GRBs. Based on detection rate of MAXI, the simultaneous detection rate of GRBs between WAM and MAXI is about 1-2 GRBs per year. In fact, we have one GRB, GRB 090831A, which is simultaneously detected by the WAM and MAXI-GSC. The long GRB 090831A triggered Suzaku WAM at 07:36:36.472 (UT) ($=T_0$) (Ohmori et al. 2009). MAXI-GSC (Matsuoka et al. 2009), Fermi-GBM (Rau et al. 2009) and many other instruments also detected this bursts. We performed a joint spectral analysis using WAM, MAXI-GSC and Fermi-GBM. Figure 8 shows the spectrum of three instruments. The spectrum of the WAM and GBM is extracted from T_0 to $T_0 + 48$ s. The MAXI-GSC spectrum is provided by the MAXI team. From WAM-GBM joint spectral fitting, the Band function with low-energy photon index α of $-1.54_{-0.05}^{+0.06}$, high-energy photon index β of < -2.2 , and the E_{peak} of 400_{-180}^{+106} keV well fit the spectrum. Figure 8 also shows this best-fit model and this model is extrapolated down to the energy range of MAXI-GSC. From this result, we found that the spectral parameters obtained by WAM-GBM joint spectral fitting also well fit the MAXI-GSC spectrum in > 10 keV band, but we can see clear residuals in softer energy band. This indicates that there is an intrinsic absorption feature in soft energy band in this GRB spectrum.

5.2. Monitoring bright sources

The WAM has capability to monitor the all-sky utilizing the earth occultation technique. Thus, we can compare the long-term light curve between soft and hard band using WAM and MAXI data. The WAM has already detected some bright hard X-ray sources such as Crab, CygX-1, GRS 1915-105, and NGC 4541. Kira et al., (2009) reported that the sensitivity of the all-sky obser-

vation by earth occultation of the WAM is 300/30 mCrab for 1-day/1-year integration, respectively. We expect that we can compare the WAM data with MAXI data in the future observations by monitoring flaring state or integrating earth occultation data for such bright sources.

6. References

- Amati, L., et al. 2002, A&A, 390, 81
- Amati, L., et al. 2006, MNRAS, 372, 233
- Atwood, W. B., et al. 2009, ApJ, 697, 1071
- Cenko, S. B., et al. 2010 ApJ, 140, 224
- de Luca, A., et al. 2010 MNRAS, 402, 1870
- Endo, A., et al. 2010 PASJ, 62, 1341
- Harmon, B. A., et al. 2002 ApJ, 138, 149
- Kira, C., et al. 2009 Proc. of 3rd MAXI workshop, 322
- Krimm, H., et al. 2009 ApJ, 704, 1405
- Matsuoka, M., et al. 2009 GCN 9852
- Meegan, C., et al. 2009 ApJ, 702, 791
- Ohmori, N., et al., 2009 GCN 9900
- Ohno, M., et al. 2005 IEEE Trans. Nucl. Sci., 52, 2758
- Ohno, M., et al. 2009 PASJ, 61, 201
- Paciesas, W. S., et al. 1999 ApJ, 122, 465
- Rau, A., et al. 2009 GCN 9850
- Sakamoto, T., et al. 2010 PASJ, in press
- Sugita, S., PhD thesis 2009
- Takahashi, T., et al. 2007 PASJ, 59, S35
- Yamaoka, K., et al. 2009 PASJ, 61, S35
- Yonetoku, D., et al. 2004, ApJ, 609, 935